FEBS Letters 473 (2000) 188–194 FEBS 23654

α-Actinin-2 couples to cardiac Kv1.5 channels, regulating current density and channel localization in HEK cells

Neil D. Maruoka, David F. Steele, Billie P.-Y. Au, Pauline Dan, Xue Zhang, Ed D.W. Moore, David Fedida*

Department of Physiology, University of British Columbia, 2146 Health Sciences Mall, Vancouver, BC, Canada V6T 1Z3

Received 28 January 2000; received in revised form 31 March 2000

Edited by Maurice Montal

Abstract Voltage-gated K^+ (Kv) channels are particularly important in the physiology of excitable cells in the heart and the brain. PSD-95 is known to cluster *Shaker* channels and NMDA receptors and the latter is known to couple through α-actinin-2 to the post-synaptic cytoskeleton [Wyszynski et al. (1997) Nature 385, 439–442], but the mechanisms by which Kv channels are linked to the actin cytoskeleton and clustered at specific sites in the heart are unknown. Here we provide evidence that Kv1.5 channels, widely expressed in the cardiovascular system, bind with α-actinin-2. Human Kv1.5 interacts via its N-terminus/core region and can be immunoprecipitated with α-actinin-2 both after in vitro translation and from HEK cells expressing both proteins. The ion channels and α-actinin-2 co-localize at the membrane in HEK cells, where disruption of the actin cytoskeleton and antisense constructs to α-actinin-2 modulate the ion and gating current density.

Key words: α-Actinin-2; K^+ channel; Kv1.5; Gating

1. Introduction

In the last decade, the role of the cytoskeleton in anchoring ion channels to regions of the membrane has been closely examined. Immunohistological studies have shown that ion channels undergo highly specialized subcellular localization at the plasma membrane which is crucial to cell function [2,3]. *Shaker*-type K^+ channels and NR2 subunits of the NMDA receptor cluster in neurons through direct linkage to a core protein of the post-synaptic density, PSD-95 [4,5], which belongs to a family of membrane-associated guanylate kinases. These homomultimerize through N-terminus linkages [6,7] and can cluster K^+ channels into plaque-like formations at the membrane (PSD-95) or intracellular aggregates (SAP97) [8,9]. Within PSD-95, repeat regions called PDZ domains facilitate ion channel localization via the distal C-termini motifs D/E-S/T-X-V of both *Shaker* and NMDA channels [10–13].

There is also indirect evidence that cardiac ion channels can be regulated by cytoskeletal interactions. Muscle Na^+ channels interact with syntrophins found in the sarcolemma and the neuro-muscular junction [14]. Syntrophins contain a PDZ domain [14] and bind dystrophin, which couples them to the actin cytoskeleton. Na^+ channel gating is directly affected by cytochalasin treatment in cardiac myocytes [15,16], which alters both channel availability and open probability. Cytochalasins accelerate cardiac ATP-sensitive K^+ channel rundown [17], attenuate sulfonylurea inhibition [18,19] and directly influence cardiac K_{IR} rectification and substrate expression [20]. In addition, Kvβ1 subunit actions on Kv1 (voltage-gated K^+) channels are modified by cytochalasins [21,22]. In this study, we show that the expression of human Kv1.5 channels in HEK cells is regulated by cytoskeletal interactions. We further demonstrate that in HEK cells the channel binds with α-actinin-2, a likely mediator of this regulation. Both disruption of the actin cytoskeleton with cytochalasin D and incubation with an α-actinin-2 antisense oligonucleotide significantly increase Kv1.5-dependent K^+ currents in Kv1.5-expressing HEK cells. Imaging experiments demonstrate cellular co-localization of Kv1.5 and α-actinin-2 which is eliminated in the presence of cytochalasin D. Finally, we show that the α-actinin-2 binding site of Kv1.5 lies in its N-terminus/core region. These results suggest a role for the actin cytoskeleton and α-actinin-2 in the organization of K^+ channels at the cell surface.

2. Materials and methods

2.1. Yeast two-hybrid library screen

A large fragment of Kv1.5 (amino acids (AA) 71–561) was subcloned in frame into the GAL4 DNA binding domain (BD) vector pGBD-C2 [23] and used to screen a pGAD10 human cardiac cDNA library (Clontech). Transformants in yeast strain PJ69-4a [23] were grown on minimal media lacking leucine and tryptophan. After 3 days growth, they were replica-plated to media lacking adenine and histidine to screen for interaction. Potential interactors were subjected to plasmid loss/retransformation tests to ensure that the resultant phenotype and reporter gene activity was plasmid-dependent. They were also tested for interaction with empty pGBD-C2 to eliminate artifactual interactions.

2.2. Analysis of protein–protein interactions by the yeast two-hybrid system

Protein–protein interactions were analyzed in two yeast strains. Growth on media lacking adenine and histidine was monitored in PJ69-4a harboring the α-actinin-2 clone isolated in the original screen. β-Galactosidase assays [24] were conducted in Y187. β-gal activity was measured spectrophotometrically at OD420 where OD = optical density. Units are: 1 β-gal unit = $1000 \times OD420/[OD600 \times \text{time (h)} \times$ volume of initial culture (ml)]. The following fragments of Kv1.5 were tested for interaction with α-actinin-2: Kv1.5 (AA 71–561), N-term (AA 1–209), N-del (AA 210–581), L-N-term (AA 71–361), S4-C-term (AA 419–561), C-term (AA 515–561) and full C-term (AA 451–614). All assays were performed on two to three different yeast transformants on several different experimental days.

2.3. Cloning and sequencing of the full-length α-actinin-2 gene

From the published sequence of α-actinin-2 in skeletal muscle and heart [23], primers for the 5′ and 3′ untranslated regions were de-

*Corresponding author. Fax: (1)-604-822 6048.
E-mail: fedida@interchange.ubc.ca

PII: S0014-5793(00)01521-0

signed and used to clone α-actinin-2 from human cardiac polyA+ mRNA (Clontech). *Kpn*I and *Eco*RI sites were engineered into the primers to facilitate subcloning.

2.4. Antisense experiments

Phosphorothioate oligonucleotides were synthesized by Operon Technologies (Alameda, CA, USA). The sequence of the α-actinin-2 antisense oligonucleotide, spanning the start codon, was CGT-GTTCATGGCGCT. The α-actinin-2 sense construct sequence was AGCGCCATGAACCAG. HEK cells were incubated with 5 μM oligonucleotide for varying time periods and then subjected to electrophysiological analysis [25]. In some experiments co-transfection with the vector pHook-1 (Invitrogen, San Diego, CA, USA) and lipofectamine was used [26]. This allowed efficient detection of transfected cells with beads coated with phOX. An α-actinin-2 antisense construct, produced by subcloning the 377 bp *Kpn*I–*Hin*dIII fragment of α-actinin-2 into *Hin*dIII–*Kpn*I-digested pcDNA3 was used in some experiments. Expression from the plasmid produces an antisense transcript spanning 309 bp of coding sequence, including the start codon, as well as 68 bp of untranslated leader.

2.5. In vitro translation

In vitro translation was carried out using the Single Tube Protein System 3, T7 (Novagen). Kv1.5 was translated from pRC/CMV/Kv1.5. α-Actinin-2 was translated from the full-length clone. Kv1.5 translation reactions included [^{35}S]methionine and were supplemented with canine pancreatic microsomes (Boehringer Mannheim).

2.6. Co-immunoprecipitations

For in vitro translations, 30 μl aliquots of in vitro-translated proteins were mixed and then 5 μl of the anti-α-actinin-2 antibody (Sigma A5044) was added. The mixtures were held on ice for 2 h and precipitated by the addition of 20 μl of pre-swelled protein A-Sepharose (Sigma). The beads were spun down and washed six times with extraction buffer (2 mM Tris–Cl, pH 8.0, 140 mM NaCl, 0.5% Triton X-100). Bound proteins were extracted by boiling in sodium dodecyl sulfate (SDS)-sample buffer for 5 min and were resolved by polyacrylamide gel electrophoresis (PAGE). The resultant gels were dried and autoradiographed. For co-immunoprecipitations from Kv1.5 and α-actinin-2 expressing HEK cells, supernatants from cell extracts [27] were employed as follows. Twenty μl of pre-swelled Sepharose CL4B in Bead Buffer (20 mM HEPES, pH 7.4, 5% glycerol, 100 mM NaCl, 0.1 mM EDTA) was added to 50 μl aliquots of the supernatant and incubated with mixing for 15 min on ice. The mixtures were spun for 15 s in a microcentrifuge and the supernatants transferred to fresh tubes. Ten μl of the appropriate antibody (buffer in control) was added to each tube and incubated on ice for 1 h with mixing. 12.5 μl pre-swelled protein A-Sepharose in Bead Buffer was added to each tube and incubated on ice for 1 h with mixing. The mixtures were spun for 15 s in the microcentrifuge and the pelleted beads were then washed three times each with wash buffer (10 mM Tris–HCl, 140 mM NaCl, 0.1% Triton X-100, 0.1% hemoglobin, 1 mM PMSF) then twice with TS buffer (10 mM Tris–HCl, 140 mM NaCl). The pellets were then each boiled in 20 μl SDS-loading buffer (0.7% Tris base, 13% glycerol, 4.9% β-mercaptoethanol, 2.3% SDS, 0.003% bromophenol blue) and subjected to PAGE. After the gels were run, they were transferred to PVDF membranes and probed as Western blots with anti-α-actinin-2 (1:300 dilution) or anti-Kv1.5 (1:250) dilution (Alomone Labs).

2.7. Mammalian cell lines

The human embryonic kidney cell line 293 (HEK-293) was used as a stable and transient expression system [28]. Cells were grown in Minimal Essential Medium at 37°C in an air/5% CO_2 incubator. One day before electrophysiological use, or transfection, cells were plated on glass coverslips in 25 mm Petri dishes with 30–50% confluence. All cell culture supplies were obtained from Canadian Life Technologies (Bramalea, Ont., Canada).

2.8. Electrophysiology

Solutions and methodology for the recording of ion and gating currents from the stable Kv1.5 cell lines are as previously reported from our laboratory [26,29]. The standard pipette filling solution contained (in mM): KCl, 135; EGTA, 5; $MgCl_2$, 1; HEPES, 10; and was adjusted to pH 7.2 with KOH. The standard bath solution contained (in mM): HEPES, 10; $MgCl_2$, 1; $CaCl_2$, 1; KCl, 5; NaCl, 135; and was adjusted to pH 7.4 with NaOH. All chemicals were from Sigma Aldrich (Mississauga, Ont., Canada). For gating currents a W472F non-conducting mutant channel was used and KCl and NaCl in the bath and pipette solutions were substituted by NMDG-Cl [29]. Coverslips containing cells were removed from the incubator before experiments and placed in a superfusion chamber (volume 250 μl) containing the control bath solution at 22–23°C. Whole-cell recordings were made using an Axopatch 200B amplifier (Axon Instruments, Foster City, CA, USA). Activation of Kv1.5 was measured on repolarization to −40 mV after 100 ms depolarizations to between −80 and +80 mV. Inactivation was measured at +60 mV after 7.5 s conditioning pulses to between −80 and +50 mV to inactivate currents. Currents were normalized to peak currents obtained at full activation and without inactivation. Data were fit to a Boltzmann function ($y = 1/(1+\exp[(V-V_{1/2})/k])+C$) where $V_{1/2}$ represents the voltage at which 50% activation or inactivation occurred, V is the membrane potential and k is the slope factor that reflects the steepness of the voltage-dependence. Lines through data points were generated with averaged parameters obtained from individual data sets.

2.9. Imaging

HEK cells were fixed in 2% paraformaldehyde for 10 min. The fixation was quenched with 100 mM glycine and the cells were permeabilized with 0.1% Triton X-100 for 10 min, rinsed 3×10 min in phosphate buffered saline and labeled for 24 h at 4°C with antibodies specific for Kv1.5 (affinity-purified polyclonal rabbit anti-rat IgG, Upstate Biotechnology) and α-actinin (monoclonal IgM, Sigma A5044). Secondary antibodies were Texas-red conjugated goat anti-mouse IgM μ-chain specific and fluorescein conjugated goat anti-rabbit (Jackson Immunobiologicals). A Nikon Diaphot 200 microscope equipped for epifluorescence with a 100/1.3 Fluor objective was used to acquire a series of 2D images through the cell at 0.25 μm intervals onto a thermoelectrically-cooled CCD camera (Tektronix TK512CB chip). Images were dark-current and background subtracted, corrected for non-uniformities across the field of view and deconvolved with an empirically determined point-spread-function using the Carrington algorithm on an EPR server (Scanalytics) [30]. Small beads which fluoresced in both wavelengths were added to the coverslips and used to align the 3D data sets. The voxels corresponding to the most likely location of the cell surface were identified utilizing an algorithm that seeks voxels which are local maxima along an intensity gradient created by convolving the deconvolved image with a small Gaussian point spread function (FWHM 4 pixels) [31]. The surface voxel in the deconvolved image and three voxels on either side, were retained for analysis, all other voxels were set to an intensity of 0.

3. Results and discussion

3.1. The yeast two-hybrid screen detects a strong interaction between Kv1.5 and α-actinin-2

An improved version [23] of the yeast two-hybrid system [32] was used to screen for protein–protein interactions with the human voltage-gated cardiac Kv channel, Kv1.5. A large fragment of Kv1.5 (AA 71–561) was subcloned in frame into a plasmid containing the DNA BD of the GAL4 protein (pGBD). This fusion protein vector, p1.5GBD was used to screen a human cardiac cDNA library (Clontech) in the GAL4 activation domain (AD) plasmid, pGAD10 in yeast strain PJ69-4A [23]. Several colonies grew on plates lacking adenine and histidine (−ade,−his), indicating activation of the reporter genes in PJ69-4A. These were subjected to plasmid loss/retransformation tests to ensure that the resultant phenotype and reporter gene activity were plasmid-dependent. Control transformations with either empty pGAD, pGBD-C2 or both, did not grow on the selective medium.

From one colony satisfying these conditions, we isolated a DNA fragment approximately 2.5 kb in length from the library plasmid. Sequencing revealed a partial (∼30%) coding region of α-actinin-2 expressed in this clone (pactGAD). The

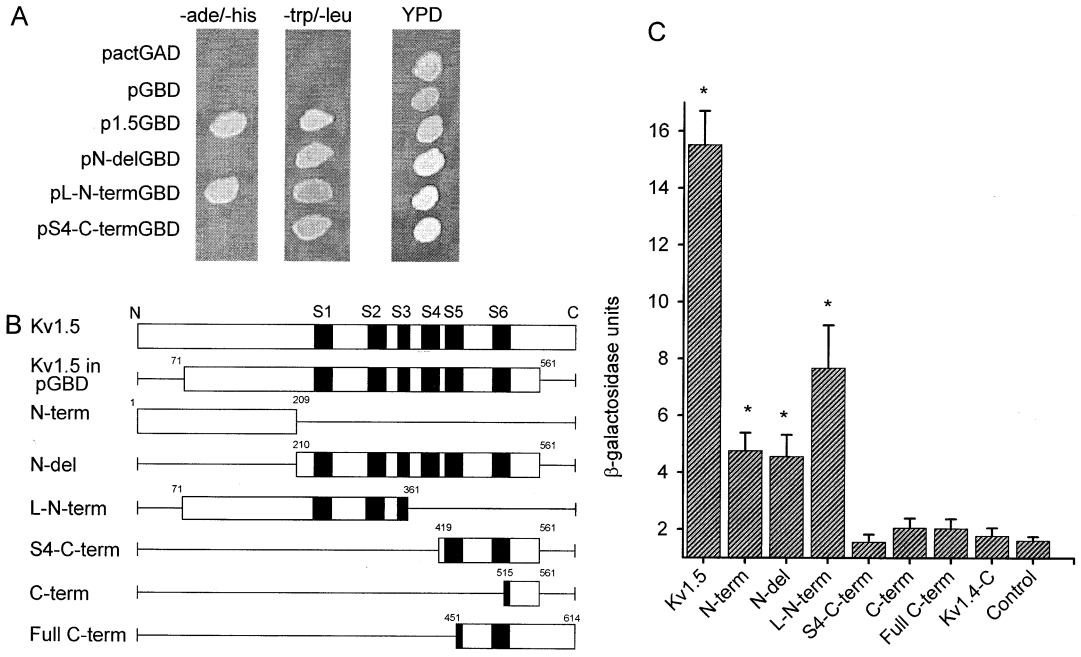

Fig. 1. Growth and β-galactosidase assays identify the interaction of Kv1.5 channels with an α-actinin-2 fragment. A: Yeast two-hybrid assay for the interaction of α-actinin-2 (AA 583–694) with Kv1.5 channel fragments. Patches were made as labeled: pGBD (control), p1.5GBD (AA 71–561), pN-delGBD (AA 210–561), pL-N-termGBD (AA 71–361), pS4-C-termGBD, (AA 419–561). All yeast except pGBD contain pactGAD. Growth on SD−trp,−leu assays for the presence of plasmids carrying the genes. Growth on SD−ade,−his indicates a detectable interaction. B: Diagrammatic representation of Kv1.5 (top) and fragments of Kv1.5 fused to the GAL4 DNA BD. Black bars denote transmembrane domains 1–6 (left to right). C: β-Galactosidase activity initiated by the interaction of Kv1.5 domains or Kv1.4 C-terminus (Kv1.4-C) subcloned into pGBD, with α-actinin-2 in pactGAD. Yeast in the control assay contained solely pactGAD. Yeast transformed with any Kv1.5 fragment/pGBD plasmid alone showed no β-gal activity higher than controls or Kv1.4 C-terminus. $n = 6$–11 for β-gal constructs. * in (C) indicate a significant difference from control, $P < 0.05$.

sequence encoded AA 583 through 694 of α-actinin-2, representing roughly half of the third spectrin repeat, the entire fourth spectrin repeat and the Ca^{2+}-binding EF-hands [33]. The incubation of yeast containing p1.5GBD and pactGAD on reporter gene selective media plates (−ade,−his) at 30°C showed significant growth over a period of 5 days (Fig. 1A).

This finding immediately suggested other yeast two-hybrid studies that have identified α-actinin-2 as a PSD protein in rat brain, directly binding to the C-terminus of both the NR1 and NR2B subunits of the NMDA receptor through its central domain spectrin repeats and immunoprecipitating with channels and PSD-95 [1]. In cultured neurons, α-actinin-2 also colocalizes with NMDA receptors at the PSD of glutamatergic synapses [34]. To further isolate the region of Kv1.5 that interacted with α-actinin-2, we subcloned a number of Kv1.5 constructs encoding N- and C-terminus regions of the subunit into pGBD (Fig. 1B). Of these, only N-terminus constructs grew on −ade,−his plates (Fig. 1A, see below) and significantly, the N-term construct co-expressed with α-actinin-2 in PJ69-4A papillated on −ade,−his media (not shown). Numerous fast-growing colonies appeared on a very slow-growing background. The growth of these papillae was plasmid-dependent and retransformation after plasmid loss returned the papillating phenotype. One explanation for this phenomenon is that the interaction requires an excess of one of the interactors. Perhaps α-actinin-2 interacts with a site that bridges two or more interacting Kv1.5 subunits, or perhaps the Kv1.5 N-terminus/GAL4 DNA BD fusions are not efficiently translocated to the yeast nucleus.

3.2. Identification of Kv1.5 fragments that interact with α-actinin-2

We targeted the C- and N-termini of Kv1.5 as potential interacting domains because of previous work with the C-terminus of NMDA channels and due to the hydrophilic and cytoplasmic nature of both termini in *Shaker*-type channels. The N-terminus of Kv1.5 is a large domain of approximately 210 AA and involved in channel assembly, β-subunit-binding and interaction with other cytoplasmic signaling proteins [35,36]. The C-terminus is shorter, approximately 100 AA in length and is a putative target for cytoskeletal proteins and regulatory kinases. We utilized the yeast two-hybrid *lacZ* reporter gene to estimate the relative strength of interaction between various domains in Kv1.5 and the α-actinin-2 interacting fragment. Several new Kv1.5/pGBD constructs were made and co-transformed with pactGAD into yeast containing a *GAL1-lacZ* reporter gene. The yeast strain Y187 was used in place of PJ69-4A, because the latter strain gave constitutive β-galactosidase activity in our hands. Seven different regions of Kv1.5 were analyzed (Fig. 1B).

The Kv1.5/GAL4 fusion construct that demonstrated strong growth in the ADE2/HIS3 reporter gene assay, also showed high levels of β-galactosidase activity. β-galactosidase activity of Kv1.5 in pGBD (Fig. 1C), in the presence of pactGAD was 15.52 ± 1.18 β-gal units ($n = 8$); control activity was 1.61 ± 0.14 β-gal units ($n = 7$). The N-terminus of Kv1.5 (N-term) also yielded significant β-galactosidase activity (4.76 ± 0.64, $n = 7$), but less than the intact Kv1.5, as did a construct in which the N-terminus of Kv1.5 was deleted (N-del). β-Galactosidase activity of this construct in the pres-

ence of pactGAD was comparable to that of the N-terminus alone (4.56 ± 0.76, $n = 6$). A construct across the boundary of these constructs (L-N-term) reconstituted more of the β-gal activity of Kv1.5 in pGBD (7.68 ± 1.5, $n = 5$). Thus, a significant portion of the interaction between Kv1.5 and α-actinin-2 is mediated across a region where the N-terminus meets the core transmembrane domains of the protein. As evidenced by the papillation noted for the N-terminus construct, some of the β-galactosidase activities reported here probably reflect the background levels of interaction and may underestimate interaction strengths in vivo.

Three C-terminus fragments of Kv1.5 were examined for interaction with α-actinin-2. None yielded *lacZ* reporter gene activity above control, showing that there is little to no interaction between the C-terminus of Kv1.5 and α-actinin-2. To confirm previous studies that excluded this region as binding α-actinin-2 [1], an additional vector was constructed, fusing the C-terminus of *Shaker*-type Kv1.4 (Kv1.4-C, AA 611–654) to the GAL4 BD. β-Galactosidase activity for the Kv1.4 C-terminus was not significantly different from control at 1.78 ± 0.28, $n = 15$. The site of interaction of α-actinin-2 appears to be near the boundary of the N-terminus with the first transmembrane domain of Kv1.5 (Fig. 1). This differentiates it from NMDA receptor/α-actinin-2 interaction and that of *Shaker* channels with other cytoskeletal proteins which are mediated through their C-termini.

3.3. Co-immunoprecipitation of α-actinin-2 and Kv1.5

After cloning and sequencing of α-actinin-2, we in vitro-translated both the full-length Kv1.5 and α-actinin-2 in rabbit reticulocyte lysate. This experiment allowed a test of direct interactions between the two proteins without the possible intercession of other proteins present in co-immunoprecipitations from cells or tissues. Kv1.5 was translated in the presence of [^{35}S]methionine and canine pancreatic microsomes and immunoprecipitated with unlabeled in vitro-translated α-actinin-2 using the anti-α-actinin antibody. When bound to protein A-Sepharose, the antibody precipitated [^{35}S]Kv1.5 (Fig. 2A, lane 1) when α-actinin-2 was present. Kv1.5 was not pulled down in the absence of α-actinin-2 (lane 2) or antibody (lane 3). This in vitro experiment has been fully confirmed in HEK cells. Using a new antibody to Kv1.5 (Transduction Labs) which detects a single band in Kv1.5-transfected HEK cells (not shown), α-actinin-2 can be efficiently co-immunoprecipitated with Kv1.5 from the HEK cell extracts (Fig. 2B,C, lane 3). Antibody to α-actinin-2 also efficiently pulls down Kv1.5 with α-actinin-2 (Fig. 2B,C, lane 2). These are detected at ~98 kDa when the Western blot was probed with the anti-α-actinin-2 antibody (Fig. 2B) and at ~68 kDa when the Western blot was probed with anti-Kv1.5 (Fig. 2C). The controls in lane 1 of Fig. 2B,C exclude non-specific actinin-2- or Kv1.5-binding to the protein A-Sepharose. These results confirm the interaction between Kv1.5 and α-actinin-2 seen in the yeast two-hybrid growth assay, both in vitro and in HEK cells.

3.4. The cytoskeleton and α-actinin-2 are important in Kv channel function

Studies on the NMDA receptor have shown that actin depolymerization reduces channel activity [37]. This led to identification of calmodulin, in competition with the actin-binding protein, α-actinin-2, as a mediator of Ca^{2+}-dependent inactivation of NMDA channels [1,38,39]. Using cytochalasin D and a stable cell line expressing Kv1.5, we examined the functional effects of coupling between the actin cytoskeleton, α-actinin-2 and Kv1 channels. Exposure to cytochalasin D for longer than 2 h caused a huge increase in ionic and gating currents through Kv1.5 channels (Fig. 3). Control ionic currents from the Kv1.5 stable line are relatively small at 200–300 pA/pF (Fig. 3A); currents in cytochalasin D-treated cells were over 700 pA/pF at 2 h and over 1000 pA/pF after incubation for longer than 24 h. A reduced but highly significant effect was also shown with the weaker actin depolymerizing agent cytochalasin B (Fig. 3B). The actions of cytochalasin D were entirely prevented by pre-incubation with phalloidin (Fig. 3B).

We used gating current measurements to test whether the observed ionic current increase resulted from an increase in the number of functional channels at the plasma membrane. Normally in this cell line the channel density at the cell surface is at the lower limit of recording of gating currents (Fig. 3C). After cyto-D for 48 h gating currents could be clearly observed and conform well to those we have observed previously from Kv1.5 [40]. Mean data from 15 cells confirmed this highly significant action (Fig. 3D). These results confirmed that at least part of the current increase was caused by more functioning channels at the cell surface, but it did not

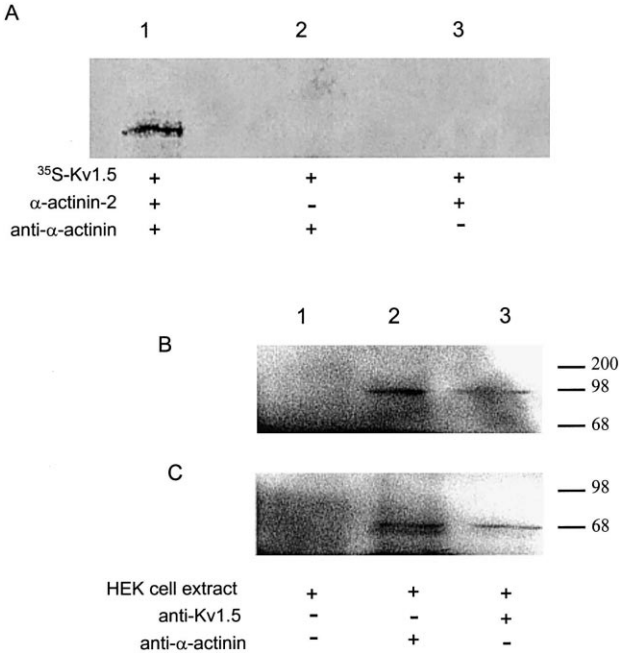

Fig. 2. Co-immunoprecipitation of Kv1.5 with α-actinin-2. A: From in vitro translation reactions. Both reactions were mixed together and immunoprecipitated using the anti-α-actinin antibody and precipitated using protein A-Sepharose (lane 1). In lane 2 immunoprecipitation is attempted in the absence of α-actinin-2 or in the absence of the antibody (lane 3). Immune complexes were resolved by SDS–polyacrylamide gel electrophoresis. B: Co-immunoprecipitation of α-actinin-2 with Kv1.5. Extracts from α-actinin-2, Kv1.5 double expressing HEK cells were mixed without antibody (lane 1), anti-α-actinin-2 (lane 2) or anti-Kv1.5 (lane 3), precipitated with protein A-Sepharose and subjected to Western analysis. The blot is probed with anti-α-actinin-2. C: Co-immunoprecipitation of Kv1.5 with α-actinin-2. The blot is identical to that in (B) except that it was probed with anti-Kv1.5. Controls (no antibody) lane 3 in (A) and lane 1 in (B) and (C) exclude non-specific binding of α-actinin-2 and Kv1.5 to the protein A-Sepharose.

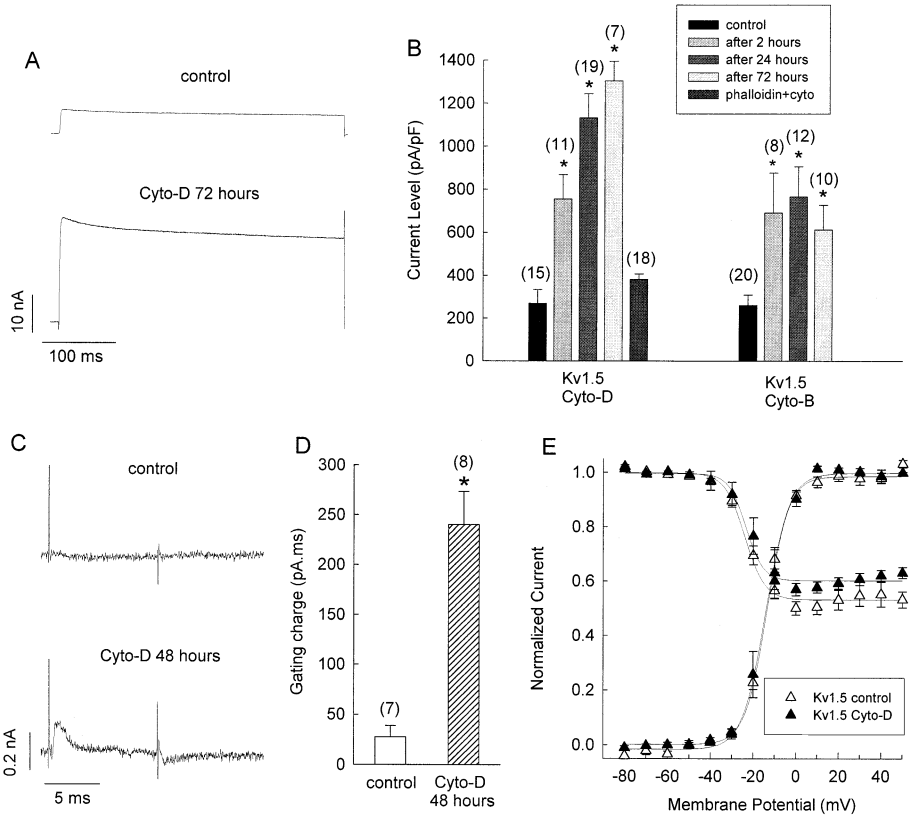

Fig. 3. Cytochalasins greatly enhance Kv channel currents in stably transfected HEK cells. A: Effect of 5 μM cytochalasin D on Kv1.5 current at +40 mV at 72 h. Cell was held at −80 mV and pulsed to +60 mV at 0.2 Hz. B: Mean data for cyto-D and cyto-B action on Kv1.5 (*n* values above bar) at different times from 2 to 72 h. Pre-incubation with 5 μM phalloidin for 5 h prevents 5 μM cyto-D action (at 24 h) on Kv1.5. * indicates a significant difference from control, one-way ANOVA, $P<0.05$. C: Gating current at +60 mV in control and after 48 h cyto-D. Cells were held at −80 mV and pulsed for 10 ms, fast transients are capacitance spikes at the start and end of voltage pulses. Data have been leak subtracted, filtered at 10 kHz and sampled at 50 kHz. D: Mean gating charge increase for 15 cells with cyto-D, * indicates difference from control, $P<0.05$. E: No effect of cyto-D on whole cell activation and inactivation kinetics for Kv1.5, symbols as indicated. Test pulse currents were normalized to the largest current amplitude, plotted against conditioning pulse potentials. Data are from 4–8 cells.

exclude the possibility that further effects occurred on the single channel open probability. However, we found no action on whole cell activation or inactivation kinetics in Kv1.5 that explained such a large current increase or that suggested modification of current kinetics after disruption of the cytoskeleton (Fig. 3E). These cytochalasin data support a potential linkage between the actin cytoskeleton and Kv1.5 channels mediated through α-actinin-2.

3.5. α-Actinin-2 antisense oligonucleotide mimics cytochalasins in its effect

In order to determine whether α-actinin-2 might mediate the interaction of Kv1.5 with the actin cytoskeleton, we carried out antisense experiments. HEK cells stably expressing Kv1.5 were incubated with 5 μM phosphorothioate α-actinin-2 antisense oligonucleotide (Fig. 4A). After 2–6 h incubation with this oligonucleotide, Kv1.5 current density was more than doubled ($P<0.05$), while incubation with α-actinin-2 sense oligonucleotide yielded no changes in Kv1.5 currents. We also transiently transfected the oligonucleotide, along with the vector pHook1 (see Section 2) and used beads to identify transfected cells at 72 h (Fig. 4B). Again, antisense incubation increased Kv1.5 between two and three times, whereas the sense oligonucleotide had little effect. Finally, the stable Kv1.5 cell line was transfected with an α-actinin-2 antisense construct in pcDNA3. This construct had qualitatively similar actions on Kv1.5 current to cytochalasins and antisense oligonucleotide incubation. Forty-eight h after transient transfection with this construct, Kv1.5 current density was doubled ($P<0.05$, Fig. 4C). Cytochalasins and antisense to α-actinin-2 both caused an increase in Kv1.5 currents. It is reasonable to infer that the increase in current seen after antisense administration may result from a disconnection of Kv1.5 from the actin cytoskeleton, associated with a reduction of α-actinin-2 in the cell.

3.6. Co-localization of Kv1.5 and α-actinin at the HEK cell surface

To further examine the functional interaction between Kv1.5 channels and α-actinin-2, HEK cells stably expressing Kv1.5 were fixed and labeled with antibodies specific for Kv1.5 and α-actinins. Images of labeled cells were obtained on a wide-field microscope and deconvolved so that the relative position of the two proteins could be assessed (Fig. 5). As the image in Fig. 5A demonstrates, both Kv1.5 and α-actinin could be seen throughout the cell, but were extensively co-localized only at the cell periphery (arrow). Peripheral co-localization was lost following pre-treatment with 5 μM cytochalasin D (Fig. 5B). This was more effectively visualized by isolating those voxels corresponding to the cell surface (Fig. 5C,D). Treated cells became more rounded and developed undulations and ruffling in the cell surface and whereas 49%

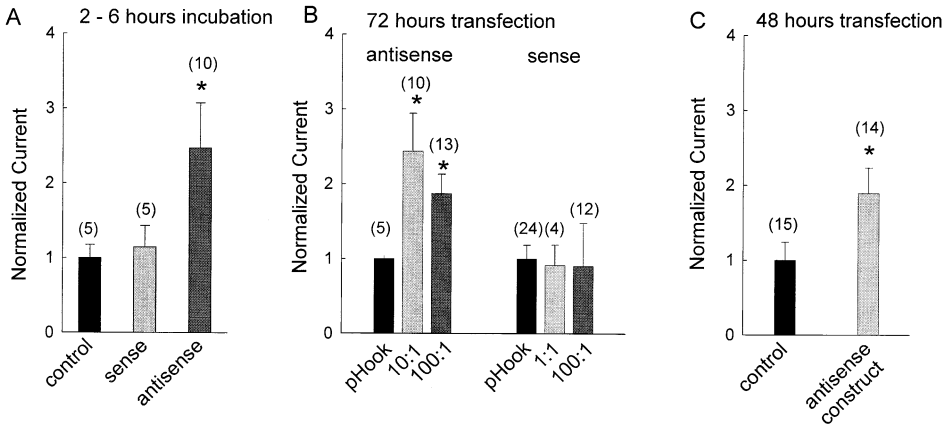

Fig. 4. Effect of α-actinin-2 antisense constructs on Kv1.5 currents. A: Kv1.5-transfected HEK cells were incubated for 2 to 6 h in 5 μM antisense or sense oligonucleotides. Mean current densities were obtained from triplicated dishes of control cells incubated in the absence or in the presence of sense and antisense oligonucleotides. Current density was normalized to control where mean Kv1.5 current density was 262 ± 46 pA/pF. B: As in (A), except that cells were transiently transfected with the oligonucleotides and the vector pHook1 plus lipofectamine. Cells were assayed for current at 72 h. Control cells (transfected with pHook alone) had a current density of 248 ± 47 pA/pF for antisense data and 396 ± 72 pA/pF for sense experiments. Cells were transfected at 1:1, 10:1 and 100:1 w:w ratios of oligonucleotide to pHook1 plasmid DNA. C: Effects on Kv1.5 ionic current of transient expression of an α-actinin-2 antisense plasmid construct into the Kv1.5 HEK stable cell line. Mean current densities were obtained from control cells (269 ± 64 pA/pF) and after 48 h transfection with lipofectamine. Transfection with empty vector had no effect on Kv1.5 currents. Number of cells examined indicated above each bar.

of the voxels identified as containing α-actinin were located at the surface in control cells, this decreased to 17% following treatment with cytochalasin D. This re-positioning of α-actinins produced a significant reduction in the extent of co-localization of Kv1.5 and α-actinin-2, which decreased from 2554 of 3876 voxels (65.9%) before, to 291 of 4121 voxels (7%) after pre-treating cells with cytochalasin D.

To summarize, we have found an interaction between a human cardiac K^+ channel and α-actinin-2, that limits the channel current measured at the HEK cell surface. We suggest that α-actinin-2 limits channel open probability or in some other way controls the functional activity or expression of channels at the cell surface. Certainly, the imaging data indicates more free Kv1.5 at the cell surface in the presence of cytochalasin D. The two possible interpretations of this observation are that the cytoskeleton, presumably through α-actinin-2, limits the density of Kv1.5 at the membrane or alters the kinetics of channels present there or both. In defining this interaction between Kv channels and the cytoskeleton, this study points the way to new regulatory mechanisms for cardiac voltage-gated ion channels, using precedents established in neurons. Conceivably, during normal electromechanical activity, cardiac Kv current density may be regulated by these cytoskeletal connections. By extension from work in

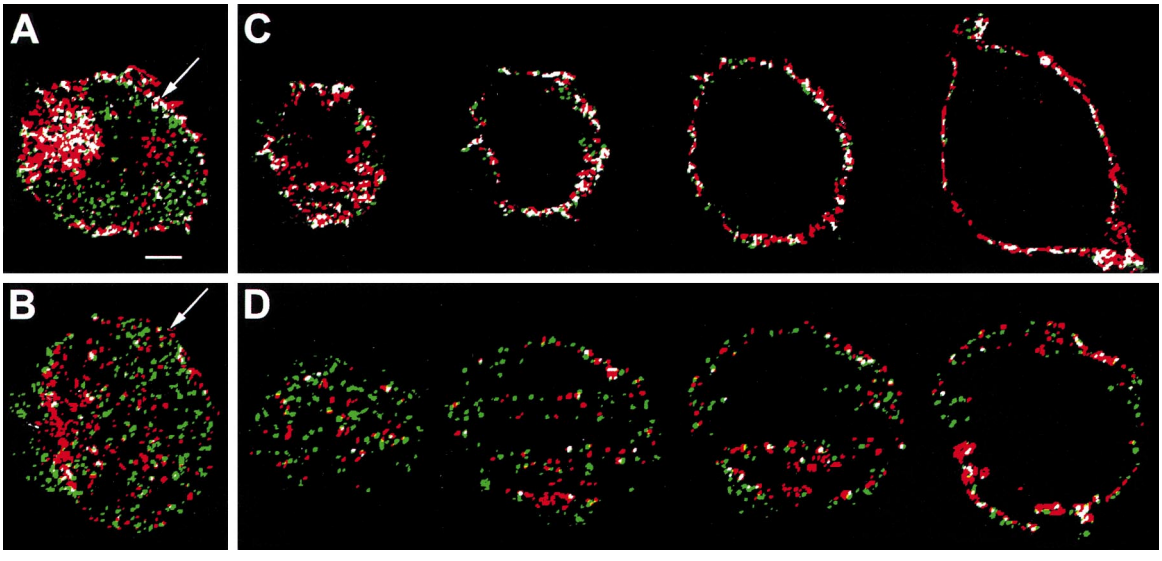

Fig. 5. Kv1.5 and α-actinin-2 co-localization in transfected HEK cells. A: Distribution of Kv1.5 (green) and α-actinin (red) in an HEK cell, voxels containing both proteins are white, optical section is 500 nm in Z, scale bar = 2.44 μm. The arrow points to the high degree of co-localization of these proteins at the cell surface. B: After treatment with cytochalasin D for 48 h. The arrow indicates little coincidence at the cell surface between Kv1.5 and α-actinin. C: The voxels corresponding to the surface of the cell were isolated and a series of 500 nm optical sections through a HEK cell, labeled as in (A), are displayed. Similar results seen in three other pairs of experiments in control and after exposure to 5 μM cytochalasin D.

neurons, the possibility also exists that these Kv channels may be regulated by Ca^{2+}, calmodulin and associated kinases [41].

Acknowledgements: Supported by grants from the Heart and Stroke Foundations of British Columbia and Yukon and the Medical Research Council of Canada to D.F. and E.D.W.M.

References

[1] Wyszynski, M., Lin, J., Rao, A., Nigh, E., Beggs, A.H., Craig, A.M. and Sheng, M. (1997) Nature 385, 439–442.
[2] Sheng, M., Tsaur, M.-L., Jan, Y.N. and Jan, L.Y. (1992) Neuron 9, 271–284.
[3] Wang, H., Kunkel, D.D., Martin, T.M., Schwartzkroin, P.A. and Tempel, B.L. (1993) Nature 365, 75–79.
[4] Cho, K.O., Hunt, C.A. and Kennedy, M.B. (1992) Neuron 9, 929–942.
[5] Kim, E., Niethammer, M., Rothschild, A., Jan, Y.N. and Sheng, M. (1995) Nature 378, 85–88.
[6] Kennedy, M.B. (1997) Trends Neurosci. 20, 264–268.
[7] Hsueh, Y.P., Kim, E. and Sheng, M. (1997) Neuron 18, 803–814.
[8] Sheng, M. (1996) Neuron 17, 575–578.
[9] Kim, E. and Sheng, M. (1996) Neuropharmacology 35, 993–1000.
[10] Kornau, H., Shenker, L., Kennedy, M.B. and Seeburg, P.H. (1995) Science 269, 1737–1740.
[11] Ziff, E.B. (1997) Neuron 19, 1163–1174.
[12] Hsueh, Y.P. and Sheng, M. (1999) J. Biol. Chem. 274, 532–536.
[13] Müller, B.M., Aarhus, R., Abbott, G.W., Abbott, N.J., Abdel-Latif, A.A., Abdel-Rahman, M.S., Abdellatif, M.M. and Abe, A. (1996) Neuron 17, 255–265.
[14] Gee, S., Madhaven, R., Levinson, S., Caldwell, J.H., Sealock, R. and Froehner, S.C. (1998) J. Neurosci. 18, 128–137.
[15] Undrovinas, A., Shander, G. and Makielski, J.C. (1995) Am. J. Physiol. 269, H203–H214.
[16] Maltsev, V. and Undrovinas, A. (1997) Am. J. Physiol. 273, H1832–H1840.
[17] Furukawa, T., Yamane, T., Terai, T., Katayama, Y. and Hiraoka, M. (1996) Pflugers Arch. 431, 504–512.
[18] Yokoshiki, H., Katsube, Y., Sunagawa, M., Seki, T. and Sperelakis, N. (1997) Pflugers Arch. 434, 203–205.
[19] Brady, P.A., Alekseev, A.E., Aleksandrov, A., Gomez, L.A. and Terzic, A. (1996) Am. J. Physiol. 271, H2710–H2716.
[20] Mazzanti, M., Assandri, R., Ferroni, A. and DiFrancesco, D. (1996) FASEB J. 10, 357–361.
[21] Jing, J., Peretz, T., Singer-Lahat, D., Chikvashvili, D., Thornhill, W.B. and Lotan, I. (1997) J. Biol. Chem. 272, 14021–14024.
[22] Levin, G., Chikvashvili, D., Singer-Lahat, D., Peretz, T., Thornhill, W.B. and Lotan, I. (1996) J. Biol. Chem. 271, 29321–29328.
[23] James, P., Halladay, J. and Craig, E.A. (1996) Genetics 144, 1425–1436.
[24] Guarente, L. (1983) Methods Enzymol. 101, 181–191.
[25] Galderisi, U., Bernardo, G., Melone, M.A.B., Galano, G., Cascino, G., Giordano, A. and Cippolaro, M. (1999) J. Cell Biochem. 74, 31–37.
[26] Fedida, D., Maruoka, N. and Lin, S. (1999) J. Physiol. (Camb.) 515, 315–329.
[27] Han, T.-H. and Prywes, R. (1995) Mol. Cell Biol. 15, 2907–2915.
[28] Fedida, D., Wible, B., Wang, Z., Fermini, B., Faust, F., Nattel, S. and Brown, A.M. (1993) Circ. Res. 73, 210–216.
[29] Wang, Z., Zhang, X. and Fedida, D. (1999) J. Physiol. (Camb.) 515, 331–339.
[30] Carrington, W.A., Lynch, R., Moore, E.D.W., Fogarty, K.E. and Fay, F.S. (1995) Science 268, 1483–1487.
[31] Lifshitz, L.M., Fogarty, K.E., Gauch, J. and Moore, E.D.W. (1992) Visual. Biomed. Comput. 1808, 521–534.
[32] Fields, S. and Song, O. (1989) Nature 340, 245–246.
[33] Beggs, A.H., Byers, T., Knoll, J., Boyce, F., Bruns, G. and Kunkel, L. (1992) J. Biol. Chem. 267, 9281–9288.
[34] Wyszynski, M., Kharazia, V., Shanghvi, R., Rao, A., Beggs, A., Craig, A.M., Weinberg, R. and Sheng, M. (1998) J. Neurosci. 18, 1383–1392.
[35] Rettig, J., Heinemann, S.H., Wunder, F., Lorra, C., Parcej, D.N., Dolly, J.O. and Pongs, O. (1994) Nature 369, 289–294.
[36] Holmes, T.C., Fadool, D.A., Ren, R. and Levitan, I.B. (1996) Science 274, 2089–2091.
[37] Rosenmund, C. and Westbrook, G. (1993) Neuron 10, 805–814.
[38] Hisatsune, C., Umemori, H., Inoue, T., Michikawa, T., Kohda, K., Mikoshiba, K. and Yamamoto, T. (1997) J. Biol. Chem. 272, 20805–20810.
[39] Krupp, J., Vissel, B., Thomas, C., Heinemann, S. and Westbrook, G. (1999) J. Neurosci. 19, 1165–1169.
[40] Chen, F.S.P., Steele, D. and Fedida, D. (1997) J. Gen. Physiol. 110, 87–100.
[41] Levitan, I.B. (1999) Neuron 22, 645–648.